^{1}H NMR Study of the Molecular and Electronic Structure of Paramagnetic Iron Chlorin Complexes of Myoglobin: Dynamic Heterogeneity of the Heme Pocket

Kelly A. Keating, Gerd N. La Mar,* Fuu-Yau Shiau, and Kevin M. Smith

Contribution from the Department of Chemistry, University of California, Davis, California 95616. *Received November 18, 1991*

Abstract: The iron complex of pyropheophorbide *a* methyl ester, **1**, and 2-devinylpyropheophorbide *a* methyl ester, **2**, have been reconstituted into equine myoglobin, Mb. The ^{1}H NMR spectra of the resulting protein complexes indicate that the chlorins are incorporated into the heme pocket in a manner similar to that of the native heme. The ^{1}H NMR spectra of the cyano-met Mb complex containing **1** and **2** are shown to be heterogeneous. In the complex of **1**, three species could be identified and labeled A, B, and C with equilibrium ratios at 5 °C of 1.0:0.4:0.04, respectively. In the complex of **2**, two species A, B in a ratio ~2:1 are detected. The equilibrium nature of the species was established by observing saturation transfer among the three species of **1** and dynamic collapse of the resonance from the two species of **2**. Assignment of the resolved resonances of the cyano metMb complex of **1** on the basis of limited isotope labeling and steady-state NOEs reveals contact shift patterns for the chromophore that are essentially identical to those of the low-spin bis-cyano model complex for the two major species, while that of the minor species C reflects a significantly altered electronic structure. The unaltered contact shift pattern for species A and B upon incorporating **1** into the protein is attributed to the fact that the rhombic perturbations due to the protein and chromophore ring saturation are co-linear and support orientation for **1** in species A and B with the 7-propionate placed as in the native protein. Conversely, the strongly perturbed contact shift pattern of species C is interpreted as reflecting an orientation of **1** with the two rhombic perturbations at right angles, indicating that **1** in C is rotated by 90° from that of A or B. The rate of interconversion among the A, B, and C species is consistent with demonstrated cases of 90° "hopping" of the heme about intact His-Fe-CN bonds. The species A and B differ primarily in the vinyl contact shift, suggesting that the orientation of the vinyl is altered by differential interactions with the protein matrix. Comparison of the presently observed heterogeneity of iron chlorophyllide complexes of Mb is made with earlier reports on related Zn^{2+} or Mg^{2+} complexes. The high-spin ferrous deoxy Mb complexes of **1** and **2** reveal a significant decrease in the axial His ring NH contact shift relative to that for hemes. Partial assignments of resonances in the deoxy Mb complex of **1** reveal extensive π spin delocalization into vacant π molecular orbitals of the chlorin. Thus a chlorin appears to serve as a better π acceptor in the high-spin ferrous states than a porphyrin. Moreover, the observations of both positive and negative delocalized π spin density can be used to rule out significant contributions to the orbital ground state from a doubly occupied d_{xy} orbital.

Introduction

Iron chlorins serve as prosthetic groups of a number of metalloenzymes such as the bacterial heme *d*[1,2] and siroheme[3,4] (an isobacteriochlorin) of sulfite and nitrite reductases; they can also be generated in situ from the heme in myoglobin, Mb, and hemoglobin, Hb, in the formation of sulfmyoglobin,[5] SMb, and sulfhemoglobin,[6] SHb. While the molecular structures of many of these chlorins are now known, the detailed electronic characteristics that result in the unique functional properties are incompletely understood. The existing data indicate that, based largely on model compounds, iron chlorins and hemes exhibit similar binding properties with respect to strong field ligands,[7,8] but the former have a greater affinity for weak-field ligand(s) and are axially more labile than iron porphyrins.[7,9] Nuclear magnetic resonance spectroscopy of paramagnetic hemes[10] in a variety of oxidation/spin states has provided a wealth of electronic/magnetic properties of the iron center as modulated by the bonding to the porphyrin and axial ligand(s). The resulting hyperfine shifts provide rich details on the environment of the active site. Most useful of the paramagnetic oxidation/spin states has been low-spin iron(III), which yields great detail on the metal-ligand π bonding, and for which the protein influence on the NMR spectral parameters of the heme yield the orientation of the His imidazole.[10,11] The unique information on the orientation of the axial ligand results because the asymmetric protein interaction resolves the essentially 4-fold symmetry of the free heme.[10-12] Conversely, the oxidation/spin state that yields the most useful information on the strength of the axial interaction is the high-spin ferrous form.[10,12,13]

In contrast to the extensive and in-depth NMR studies on iron porphyrins,[10,12] relatively few NMR studies of iron chlorin model compounds have been reported.[7,9,14,15] Several reports on in-

(1) Lemberg, R.; Barret, J. *Cytochromes*; Academic Press: New York, 1978; pp 233-345.
(2) Timkovich, R.; Cork, M. B.; Gennis, R. B.; Johnson, P. Y. *J. Am. Chem. Soc.* **1985**, *107*, 6069-6075.
(3) Murphy, M. J.; Siegel, L. M.; Tover, S. R.; Kamin, H. *Proc. Natl. Acad. Sci. U.S.A.* **1974**, *71*, 612-616. Lancaster, J. R.; Vega, J. M.; Kamin, H.; Orme-Johnson, N. R.; Orme-Johnson, W. H.; Kruger, R. H.; Siegel, L. M. *J. Biol. Chem.* **1979**, *254*, 1268-1272.
(4) Scott, A. I.; Irwin, A. J.; Siegel, L. M.; Schoolery, J. N. *J. Am. Chem. Soc.* **1978**, *100*, 316-318. Siegel, J. M.; Rueger, D. C.; Barber, M. J.; Krueger, R. J.; Orme-Johnson, N. R.; Orme-Johnson, W. H. *J. Biol. Chem.* **1982**, *257*, 6343-6350. McRee, D. E.; Richardson, D. C.; Richardson, J. S.; Siegel, L. M. *J. Biol. Chem.* **1986**, *261*, 10277-10281.
(5) Berzofsky, J. A.; Peisach, J.; Alben, J. O. *J. Biol. Chem.* **1972**, *247*, 3774-3782. Berzofsky, J. A.; Persach, J.; Horecker, B. L. *J. Biol. Chem.* **1972**, *247*, 3783-3791.
(6) Park, C. M.; Nagel, R. L.; Blumberg, W. E.; Peisach, J.; Magliozzo, R. A. *J. Biol. Chem.* **1986**, *261*, 8805-8810.
(7) Strauss, S. H.; Silver, M. E.; Ibers, J. A. *J. Am. Chem. Soc.* **1983**, *105*, 4108-4109.
(8) Stolzenberg, A. M.; Strauss, S. H.; Holm, R. H. *J. Am. Chem. Soc.* **1981**, *103*, 4763-4778. Strauss, S. H.; Holm, R. H. *Inorg. Chem.* **1982**, *21*, 863-868.
(9) Licoccia, S.; Chatfield, M. J.; La Mar, G. N.; Smith, K. M.; Mansfield, K. E.; Anderson, R. R. *J. Am. Chem. Soc.* **1989**, *111*, 6087-6093.
(10) La Mar, G. N.; Walker, F. A. *The Porphyrins*; Dolphin, D., Ed.; Academic Press: New York, 19xx; Vol. IVB, pp 61-157.
(11) Shulman, R. G.; Glarum, S. H.; Karplus, M. *J. Mol. Biol.* **1971**, *57*, 93-115.
(12) La Mar, G. N. In *Biological Applications of Magnetic Resonance*; Shulman, R. G., Ed.; Academic Press: New York, 1979; pp 305-343.
(13) Nagai, K.; La Mar, G. N.; Jue, T.; Bunn, H. F. *Biochemistry* **1982**, *21*, 842-847.
(14) Strauss, S. H.; Pawlik, M. J. *Inorg. Chem.* **1986**, *25*, 1921-1923. Strauss, S. H.; Long, K. M.; Magerstädt, M.; Gansow, O. *Inorg. Chem.* **1987**, *26*, 1185-1187.
(15) Pawlik, M. J.; Miller, R. K.; Sullivan, E. P.; Levstik, M. A.; Almond, D. A.; Strauss, S. H. *J. Am. Chem. Soc.* **1988**, *110*, 3007-3012. Sullivan, E. P.; Grantham, J. D.; Strauss, S. H. *J. Am. Chem. Soc.* **1991**, *113*, 5264-5270.

0002-7863/92/1514-6513$03.00/0

termediate-spin ferrous[14] and high-spin ferric[15] synthetic chlorin derivatives have appeared. In a single study on a natural chlorin derivative, the iron complex of the methyl ester of pyropheophorbide *a*, **1**, detailed assignment of the low-spin ferric complex revealed that while the dominant bonding involved the same filled π molecular orbital as for a heme[10,11] significant π bonding also occurs in a chlorin with the former nonbonding a_{1u} orbital of the heme, as had been previously proposed.[16] Moreover, it was concluded[9] that the spin distribution of the highest $3e_\pi$ orbital reflected a large rhombic contribution due to the saturation of a pyrrole which places the unpaired spin on the periphery primarily in the pyrroles cis to the saturated ring. To date, there has not appeared a report that considers the influence of a protein environment on the ^{1}H NMR spectral features of a paramagnetic natural metallochlorin. Such studies could aid in the interpretation of the NMR spectra of native iron chlorin proteins.[17]

Several diamagnetic chlorins containing Mg^{2+} or Zn^{2+} have been reconstituted into sperm whale apo Mb[18,19] and the products characterized by optical, CD, and ^{1}H NMR spectroscopy. Clean 1:1 chlorin:Mb complexes could be prepared, and the upfield ring current shifted E7 Val signals interpreted in terms of a single orientation of the chlorin that has the propionate side chain at the same position as for natural protohemin. However, several of the reconstituted complexes exhibited a labile heterogeneity which was attributed[19] to a minor conformational equilibrium involving heme pocket side chains, as opposed to alternate orientations of the chlorin in the pocket.

In this report, we extend our NMR studies of **1** as reconstituted into a protein matrix. Our interests are to elucidate the influence of a protein environment on the NMR spectral parameters of the low-spin ferric state and to characterize the reduced or high-spin ferrous state in an iron chlorin. As a reference protein we select equine myoglobin, Mb, for which there exists a high resolution crystal structure[20] and a complete range of detailed NMR studies of the various paramagnetic complexes of natural porphyrins in the isostructural sperm whale protein.[10,12,21] Questions that we will address are the following: Does the iron chlorin incorporate into the protein matrix in a unique manner? What are the effects of incorporation into the protein matrix on the low-spin ferric state? What is the nature of axial His bonding for an iron chlorin versus an iron porphyrin? What are the bonding properties of high-spin iron chlorin compared to those of iron porphyrin?

Experimental Section

Materials. The iron(III) complex of pyropheophorbide *a* methyl ester[22] (**1**), its complex deuterated[23] ~95% at the 5-methyl, ~90% at the γ-*meso*-methylene and ~20% at the δ-*meso*-H, and 2-devinylpyropheophorbide *a* methyl ester[24] (**2**) were prepared as described earlier. The >95% purity of **1** and **2** was established by the ^{1}H NMR spectra in the bis-cyano iron(III) complex in DMSO-$^2H_6$/^2H_2O solution, as reported[9] in detail for **1**. Attempts to de-esterify the methyl ester of the iron complex of **1** by standard procedures invariably led to degradation of the macrocycle, as reflected in the appearance of a large and varied set of altered peaks in the ^{1}H NMR spectrum. Since protohemin dimethyl ester can be incorporated into apo myoglobin, apo Mb, with essentially conserved heme pocket structure,[25] further work was restricted to the chlorin methyl esters, **1** and **2**. ApoMb was prepared from commercial (Sigma) equine skeletal Mb by standard procedures.[26]

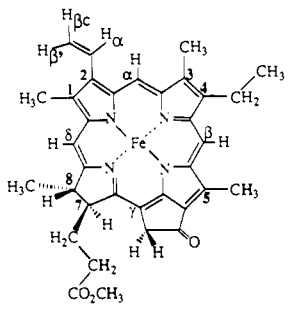

1

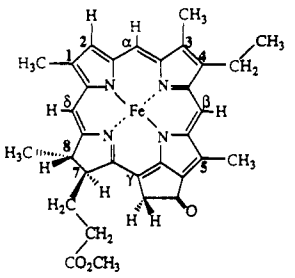

2

Reconstitution. The reconstitution of equine apoMb with **1** and **2** and the selectively deuterated isomer of **1** was performed according to the methods reported by Wright and Boxer[18] for Zn^{2+} and Mg^{2+} chlorophyllide derivatives. ApoMb(3–4 mM) was prepared[26] in ^1H_2O, 0.1 M in phosphate buffer, pH 7.0 (confirmed by optical absorption at 280 nm with ϵ = 15.2 mM^{-1} cm^{-1}). The pH was measured on a Beckman pH meter with an Ingold microcombination electrode. A solution of **1** or **2** was prepared in 6:5 pyridine/^1H_2O (50–60 μL per mg of **1** or **2**) in the presence of a ~5-fold molar excess NaCN; both the pyridine and cyanide are necessary for dissolving the complexes. The apoMb was diluted in 0.1 M phosphate buffer so that the added solution of **1** or **2** resulted in less than 5% pyridine for the reconstituted protein. The solution of **1** or **2** was slowly added at 5 °C with constant stirring and the pH monitored and adjusted with HCl as necessary to remain between 5.5 and 8.0. Optical monitoring of the reconstitution failed to yield a clear break point indicating a 1:1 ApoMb:chlorin ratio, and generally a 20% excess of chlorin was added.

The reconstituted protein solution was loaded on a Sephadex G25 column (phosphate buffer, pH 7.0) at 4 °C to remove the pyridine. As suggested by Boxer and Wright,[18] excess chlorin was removed by ion exchange chromatography with 10 mM phosphate buffer at pH 6.3 on a column of CM-Sephadex C-25-120 and eluted with 20 mM phosphate buffer, pH 7.6. The dark green product exhibited an optical spectrum with λ = 424, 666 nm. The resulting solution was concentrated and exchanged with ^2H_2O in an Amicon ultrafiltration cell to a final concentration of 2–3 mM of the metMbCN complex of **1** and **2**.

The high-spin ferrous or deoxy Mb complexes of **1** and **2** were prepared directly from the metcyano complexes by addition of a 2 M excess of dithionite to a degassed solution. The reduction is reflected in a change to a lime green color (λ = 422, 660 nm).

Spectroscopy. Optical spectra were recorded at ambient temperature in 1 cm light path quartz cells on a Hewlett-Packard 8540A UV–vis spectrophotometer. The *g* values for the metMbCN complex of **1** were obtained at 20 K on a Bruker ER 200D spectrometer at 9.5 GHz (X-band) with a field modulation of 5 G.

^{1}H NMR spectra were recorded on a Nicolet NT 360 (360 MHz) and General Electric Ω300 (300 MHz) and Ω500 (500 MHz) spectrometers, all operating in the quadrature mode. Typical spectra were obtained with 5–10 × 10^3 transients of 8192 real data points over a 50 KHz (300 or 360 MHz) or 70 KHz (500 MHz) band width using a 6–7 μs (300 or 360 MHz) or 12–14 μs (500 MHz) 90° pulse. The residual water signal was suppressed by a presaturating decoupler pulse. All chemical shifts are in ppm referenced to 2,2-dimethyl-2-silapentane-5-sulfonate (DSS). Peak areas were determined using the peak simulation computer program NMCCAP, part of Nicolet NMC software, on a Nicolet 1280 computer. T_1 values were determined by the inversion-recovery experiment using 2000 transients, with a nonselective composite 180° pulse. The T_1 values were determined from the initial slope of the plot of ln $((I_\infty - I_\tau)/2I_\infty)$ vs time or, in cases of poorly resolved peaks or very short T_1s (<10 ms), estimated from the null-point of a plot of I_τ vs time with $T_1 = \tau_{null}/\ln 2$. Reproducibility of T_1 values is ±20%.

1D nuclear Overhauser effect,[27] NOE, difference spectra were generated by subtracting a reference trace with the decoupler well off-resonance from the proton of interest from a trace where the decoupler pulse is on-resonance at the frequency of the proton of interest. The spectra were recorded using the WEFT sequence[28] with a 80-ms decoupler pulse and a pulse repetition rate of 5 s^{-1}. For the low-spin ferric metMbCN complex, the spectra required 8–10 × 10^3 scans, while the high-spin ferrous deoxy Mb complex required ~1–2 × 10^4 scans. In order to differentiate NOEs from off-resonance saturation, the decoupler fre-

(16) Hanson, L. K.; Chang, C. K.; Davis, M. S.; Fajer, J. *J. Am. Chem. Soc.* **1981**, *103*, 663–670. Chang, C. K.; Hanson, L. K.; Richardson, P. F.; Young, R.; Fajer, J. *Proc. Natl. Acad. Sci. U.S.A.* **1981**, *78*, 2652–2656.
(17) Timkovich, R.; Cork, M. S. *Biochemistry* **1982**, *21*, 5119–5123.
(18) Boxer, S. G.; Wright, K. E. *J. Am. Chem. Soc.* **1979**, *101*, 6791–6974.
(19) Wright, K. E.; Boxer, S. G. *Biochemistry* **1981**, *20*, 7546–7556.
(20) Evans, S. V.; Brayer, G. D. *J. Biol. Chem.* **1988**, *263*, 4263–4268.
(21) Satterlee, J. D. *Annu. Rept. NMR Spectrosc.* **1986**, *17*, 79–178.
(22) Kenner, G. W.; McCombie, S. W.; Smith, K. M. *J. Chem. Soc., Perkins Trans. 1* **1973**, *2517–2523*. Smith, K. M.; Fujinari, E. M.; Langry, K. C.; Parish, D. W.; Tabba, H. D. *J. Am. Chem. Soc.* **1983**, *105*, 6638–6646. Smith, K. M.; Goff, D. A.; Simpson, D. J. *J. Am. Chem. Soc.* **1985**, *107*, 4944–4954.
(23) Fajer, J.; Fujita, I.; Davis, M. S.; Forman, A.; Hanson, L. K.; Smith, K. M. *Adv. Chem. Ser.* **1982**, *1201*, 489–513.
(24) Smith, N. W. Ph.D. Dissertation, University of California, Davis, 1990.
(25) Tamura, M.; Asakura, T.; Yonetani, T. *Biochem. Biophys. Acta* **1973**, *295*, 467–479.
(26) Teale, F. W. S. *Biochem. Biophys. Acta* **1959**, *35*, 543.
(27) Neuhaus, D.; Williamson, M. *The Nuclear Overhauser Effect in Structural and Conformational Analysis*; VCH Publishers: New York, 1989.
(28) Gupta, R. K. *J. Magn. Reson.* **1976**, *24*, 461–465.

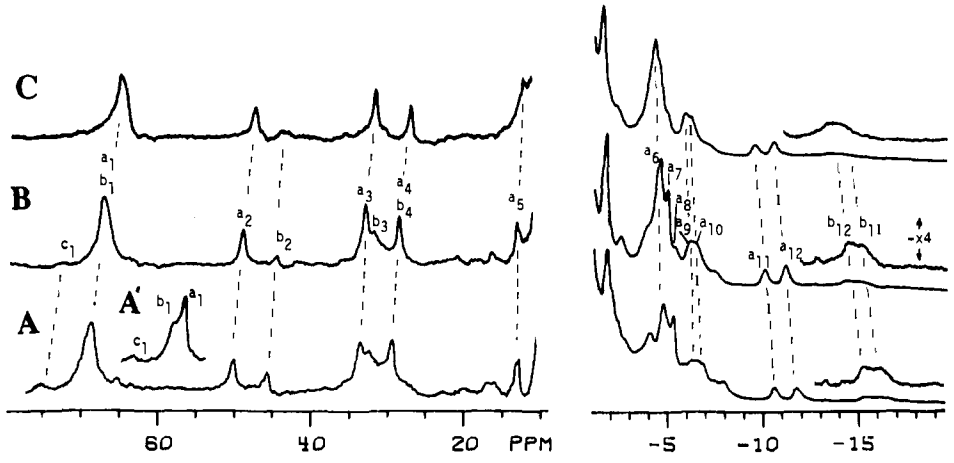

Figure 1. 360-MHz ^1H NMR spectra of a ~2 mM solution of the metMbCN complex of **1** in ^2H_2O in 0.1 M phosphate, pH 7.0, at (A) 15 °C, (B) 25 °C, and (C) 35 °C. The inset (A') shows the low-field peak at 5 °C. The resonances are labeled a_i, b_i for the two major species A and B, respectively. Nonreproducible impurity peaks are labeled by an asterisk.

quency in the reference trace was placed symmetrical with respect to the on-resonance saturating pulse about the signal giving rise to a NOE.

Saturation transfer between resonances of interconverting equilibrium species is observed in difference spectra based on the same experiment as for the 1D NOE. The intensity of the resonance i experiencing saturation, upon saturating j, is given by the saturation factor $F_i = I_i/I_i(0) = k_{ij}/(k_{ij} + T_{1i}^{-1})$, where I_i, $I_i(0)$ are the intensities of peak i with and without saturating j, respectively, k_{ij} is the rate of interconversion, and T_{1i} is the spin–lattice relaxation time of i. Determination of I_i, $I_i(0)$, and T_{1i} yields the interconversion rates.

2D data sets on the metMbCN complex of **1** were collected on the General Electric Ω-300 spectrometer. Magnitude COSY[29] was recorded over a band width of 32 258 Hz with 256 t_1 blocks of 2560 scans each of 1024 complex data points at a repetition rate of 9 s^{-1}; the solvent signal was saturated in the interpulse delay. The data were apodized with a 0° phase-shifted sine-bell function, zero-filled to 1024 in the t_1 dimension, and symmetrized. The NOESY (and EXSY) data[27] were collected over a 71 428 Hz band width with 256 t_1 blocks of 3456 scans each with 2018 complex points at a repetition rate of 11 s^{-1}; the solvent signal was saturated during the interpulse delay. Consistent with T_1s in the range 10–30 ms, a mixing time of 15 ms was used. The data were processed with a 10° phase-shifted sine-bell squared window over a 7-ms acquisition time in the t_2 dimension and zero-filled to 2048 × 2048 points prior to Fourier transformation. Neither map revealed extensive cross peaks from resolved resonances.

Results

Cyano Metmyoglobin Complexes. (a) Magnetic Properties. The ESR spectrum at 20° revealed g values of 2.81, 2.65, and 1.43, which are very similar to those of other low-spin ferric chlorin complexes.[30,31] The reduced magnetic anisotropy is indicative of a larger splitting of the orbital sublevels as compared to an isoelectronic hemin and also accounts for a longer electron relaxation time and hence broader ^1H resonances.[10]

(b) Molecular Heterogeneity. The 360-MHz ^1H NMR traces of the metMbCN complex of **1** in ^2H_2O at three temperatures are illustrated in spectra A–C of Figure 1. It is apparent in Figure 1 that there are several species in solution such that the protein sample must be heterogeneous. Thus, while the dominant set of resonances at 35° reveals an intensity pattern of three–proton peaks (a_1,a_6) and one-proton peaks (a_i with i = 2–5, 9–12), lowering the temperature reveals the appearance of weaker resonances such at these labeled b_2, b_{11}, b_{12}. The low-field methyl peak similarly exhibits a splitting at 5 °C (inset to Figure 1C). We classify the resonances as follows: completely reproducible peaks from the major species A of each reconstitution are designated a_i and exhibit relative intensities of one (single proton) or three

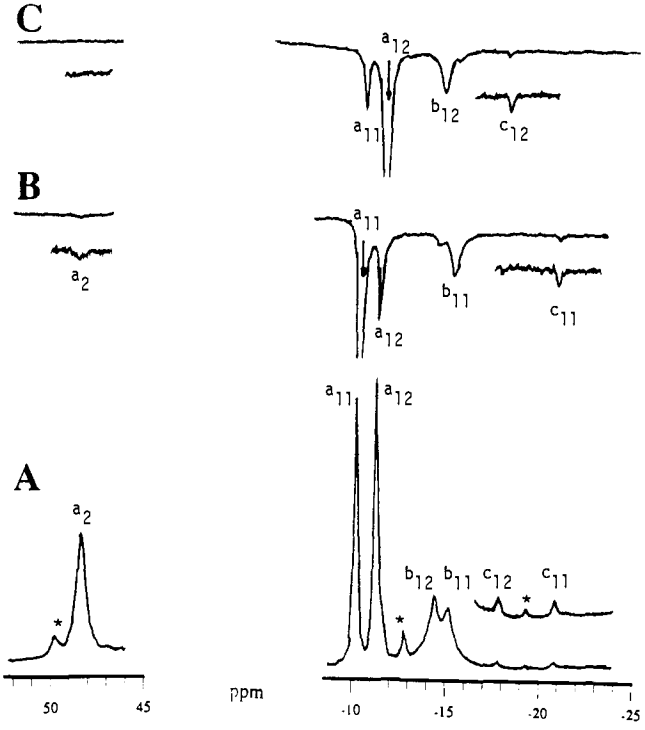

Figure 2. (A) Portions of the reference trace of the metMbCN complex of **1** at 25 °C which contain the vinyl resonances; peak labels are a_i, b_i, c_i for the three species A, B, and C, respectively; nonreproducible impurities are marked by asterisks. Note the three sets of resonances (a_{11},a_{12}), (b_{11},b_{12}), and (c_{11},c_{12}) with relative areas ~1.0:0.4:0.04. (B) Saturate peak a_{11} (arrow); note saturation transfer to b_{11} and c_{11}, as well as strong NOE to a_{12} and weak NOE to a_2. (C) Saturate peak a_{12} (arrow); note saturation transfer to both beaks b_{12} and c_{12} as well as strong NOEs to a_{11}.

(methyl group). A second set of resonances (approximate relative intensity 0.4 when compared to a_i at 5 °C) with constant relative intensities among themselves exhibits increased intensity at lower temperature and is designated b_i for species B. The components a_4,b_4 are apparently degenerate, as dictated by the intensity of the composite resonance; the pair a_3,b_3 resonate within 1 ppm of each other. The region 0 to −8 ppm also reveals more intense peaks at lower temperature, but the overlapping resonance precludes analysis. Hence we restrict ourselves to defining the heterogeneities for the clearly resolved peak outside the window 20 to −10 ppm.

Inspection of the optimally resolved upfield region reveals the presence of a third set of minor component peaks, as shown in Figure 2A; the pair of peaks c_{11},c_{12}, with intensity 0.04 compared to a_{11},a_{12}, occur in every sample and can be shown to originate

(29) Bax, A. *Two Dimensional Nuclear Magnetic Resonance in Liquids*; D. Reidel Publishing Co.: Dordrecht, Holland, 1982.
(30) Muhoberoc, B. B.; Wharton, D. B. *J. Biol. Chem.* **1983**, *258*, 3019–3027. Muhoberac, B. B. *Arch. Biochem. Biophys.* **1984**, *233*, 682–697.
(31) Berzofsky, J. A.; Peisach, J.; Blumberg, W. E. *J. Biol. Chem.* **1971**, *246*, 3367–3377.

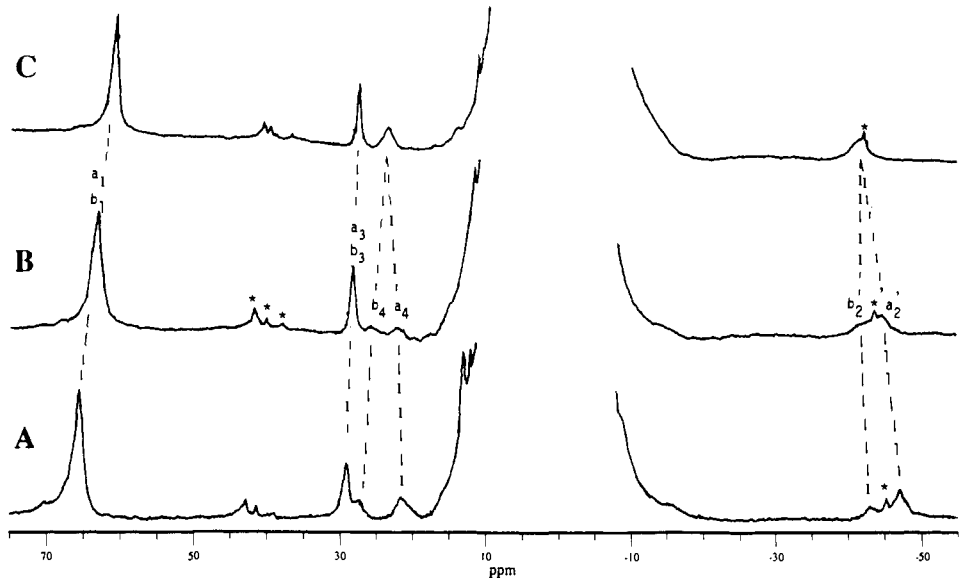

Figure 3. 360-MHz ^{1}H NMR spectra of a ~2 mM solution of the metMbCN complex of **2** in ^2H_2O, 0.1 M phosphate, pH 7.0, at (A) 25 °C, (B) 35 °C, and (C) 45 °C. Peaks are labeled a_i and b_i for the component species A and B, respectively. Apparent impurity peaks are marked by asterisks.

from a third equilibrium species from the protein which we designate C. The c_i peaks analogous to the low-field a_i,b_i peaks are not immediately apparent but can be identified via interconversion among the species (see below). The three sets of resonances a_i, b_i, and c_i, representing species A, B, and C, respectively, are observed in all reconstituted samples and represent equilibrium molecular heterogeneity. Additional multiple weak resonances representing minor components of complexes of **1**, whose intensities are highly variable with preparation but do not change with time, are detected in the ^{1}H NMR spectra. Annealing the protein (25 → 45 → 25 °C) failed to change intensity ratios, and chromatography of the sample failed to remove these peaks completely. We attribute these species, in part, to minor impurities in **1** and, in part, to nonequilibrium forms of bound **1** where the chlorin binds outside the heme cavity. We label the resonances from these impurity and nonequilibrium species with asterisks and do not consider them any further.

The ^{1}H NMR traces at several temperatures of the metMbCN complex of **2**, which has the vinyl in **1** replaced by a hydrogen, are shown in Figure 3; impurity peaks are labeled by an asterisk. At 45 °C (Figure 3C), the three resolved low-field resonances exhibit the expected 3:1:1 intensity, in analogy with the (a_1,b_1), (a_3,b_3), (a_4,b_4) resonances in Figure 1; the absence in Figure 3 of peaks at 45 ppm (a_2,b_2) and ~−10 ppm (a_{11},b_{11}), (a_{12},b_{12}) seen in Figure 2 points to their origin as the 2-vinyl H_α and H_βs in the complex of **1**. Moreover, the new upfield peaks a_2',b_2' in Figure 3 must arise from the pyrrole 2-H of **2**. Note as the temperature is lowered, the resonances at 27 and −45 ppm split into two components which we label a_i for the major and b_i for the minor equilibrium form. The intensities of the resonances at 65 ppm (labeled a_1,b_1) and ~28 ppm (labeled a_3,b_3) dictate that each is a composite.

(c) Interconversion of Equilibrium Isomeric Forms. Saturation transfer experiments[32] (or 2D EXSY; not shown) not only establish the equilibrium nature of the three isomeric species of **1** in solution but also aid in the location of the remaining of the resonances (c_i) of the species C in the resolved spectral window. The results are illustrated most clearly for the relatively uncrowded upfield spectral window shown in Figure 2A. Saturation of a_{11} yields partial saturation of both peaks b_{11} and c_{11} (Figure 2B); irradiation of peak a_{12} produces a similar effect on peaks b_{12} and c_{12} (Figure 2C). Since peaks a_i, b_i, and c_i arise from different molecular species, as dictated by their intensity ratios, the magnetization transfer must occur by saturation transfer via chemical exchange among the species A, B, and C. The saturation transfer experiments that identify the analogous set of low-field peaks are shown in Figure 4. For the low-field methyl, peaks a_1 and b_1 are too close to saturate separately (inset Figure 1A). However, irradiation of the a_1, b_1 composite reveals saturation transfer to the third minor component peak c_1 (Figure 4B). While peak c_1 is too close to peak a_1,b_1 to avoid off-resonance saturation of peak c_1, the placement of the decoupler in the reference trace symmetrical to peak c_1 cancels the off-resonance effect to peak c_1 and confirms direct magnetization transfer from peaks a_1,b_1 to c_1. Similarly, saturation of the resolved peak a_2 clearly results in the expected saturation transfer to peak b_2, but it also reveals the location of peak c_2 (Figure 4C) which is difficult to detect between the a_3 and a_4 composite in the reference trace. Saturation of the nearly degenerate a_3,b_3 peaks (Figure 4D) and degenerate a_4,b_4 (Figure 4E) each locate a peak (c_3,c_4, respectively) from species C via saturation transfer. The crowded spectral window 0 to −8 ppm did not allow tracing the minor component peak in a similar fashion.

The measured saturation factors of ~0.7 for b_{11} and c_{11} upon saturating a_{11}, together with a nonselective T_1 (8 ms for b_{11},c_{11} is too weak to yield T_1), yield ~50 s^{-1} interconversion[32] rates. Upon raising the temperature above 30 °C, peaks b_{11},b_{12} and c_{11},c_{12} lose some intensity and broaden extensively, indicating the onset of fast chemical exchange (Figure 1C). In the metMbCN complex of **2**, the NMR spectra in Figure 3 clearly show that the pairs of resonances a_4,b_4 and a_2',b_2' each dynamically collapse to yield averaged resonances at 45 °C (Figure 3C). A set of peaks analogous to the third component C was not identified for the complex of **2**. Moreover, since similarly separated resonances (by ~5 ppm) are still resolved in the complex of **1** at 35 °C (peaks a_{11},a_{12} and b_{11},b_{12}) but are in the intermediate exchange in the complex of **2** (peaks a_2',b_2'), the interconversion between species A and B is faster for **2** than **1**.

(d) Resonance Assignment. Reconstitution with **1** that has its 5-CH_3, γ-*meso*-CH_2, and δ-*meso*-H deuterated[23] yields a metMbCN trace with only peaks a_1,b_1 missing among resolved resonances (not shown). Hence signals a_1,b_1,c_1 must originate from the 5-CH_3. Comparison of the metMbCN trace of **1** (Figure 1A,B,C) and **2** (Figure 3A,B,C) dictates that the sets (a_2,a_{11},a_{12}), (b_2,b_{11},b_{12}), and (c_2,c_{11},c_{12}) of **1** arise from the 2-vinyl group, with a_2,b_2,c_2 as the H_α, and resonances a_2',b_2' of **2** arise from the 2-H. The resonances of the bis-cyano complex of **1** and **2** are essentially identical except for the 2-position (supplementary material). Moreover, the positions of resolved resonances in the bis-cyano model and metMbCN complex of both **1** and **2** are also strikingly similar (Table I).

(32) Sandström, J. *Dynamic NMR Spectroscopy*; Academic Press: New York, 1982; Chapter 2.

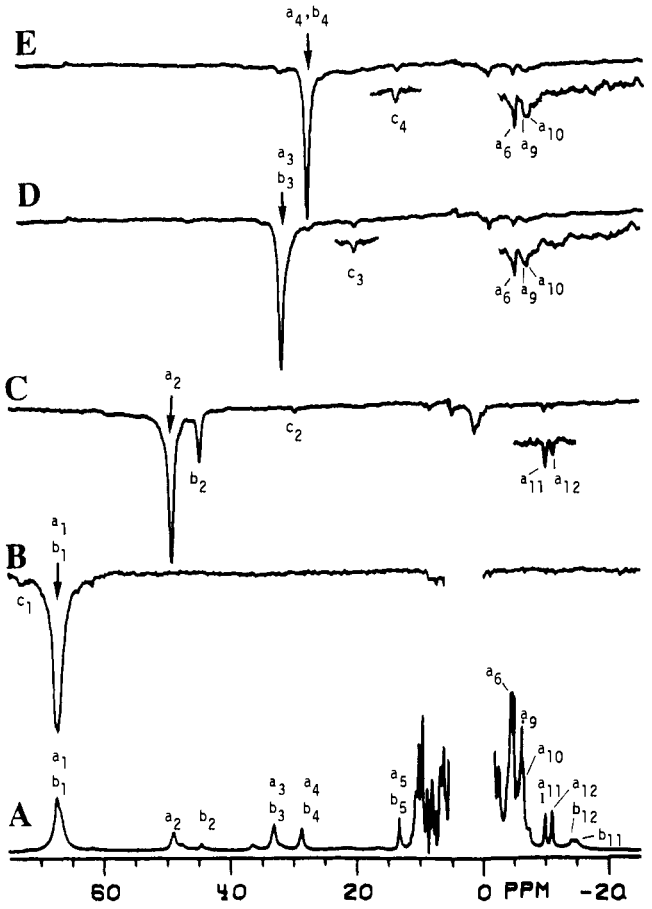

Figure 4. (A) Reference trace of the metMbCN complex of **1** in ^2H_2O, at 25 °C, 0.1 M phosphate, pH 7.0, with peaks labeled a_i for the major species A. (B–E) NOE/saturation-transfer difference traces obtained by saturating the resonance marked with a vertical arrow and subtracting the trace from one with the decoupler placed well off-resonance; the position of the off-resonance decoupler is marked by a triangle. (B) Saturate 5-CH_3 composite peak a_1,b_1; note the saturation transfer to peak c_i and absence of detected NOEs outside the diamagnetic window; the decoupler in the reference trace is symmetrical with respect to c_1. (C) Saturate peak a_2; note the saturation transfer to both peaks b_2 and c_2, as well as NOEs to a_{11} (2-$H_{\beta c}$) and a_{12} (2-H_{Bt}). (D) Saturate composite resonance a_3,b_3; note the saturation transfer to peak c_3, as well as NOEs to methyl a_6 (8-CH_3) and peaks a_9,a_{10} (7-H_αs). (E) Saturate composite peak a_4,b_4; note the saturation transfer to peak c_4 as well as NOEs to a_6 (8-CH_3) and a_9,a_{10} (7-H_αs). The resonances c_2, c_3, and c_4 are too weak to label in the reference trace.

A magnitude COSY map[29] yielded but one detectable cross peak involving a resolved resonance (not shown), that between peaks a_2 and a_{12}, which dictates that the two protons arise from the most strongly spin coupled pair on **1**, the 2-H_α and 2-$H_{\beta t}$, respectively. Extensive cancellation of the antiphase cross peaks due to the large line widths precludes detection of the cross peaks for the more weakly coupled spins. A NOESY map yields similarly limited data because of the relatively low concentration of the sample and rapid relaxation rates of resolved resonances (not shown). However, some assignment could be pursued effectively by 1D steady-state NOEs.[27,33] Saturation of a_{11} but not a_{12} yields an NOE to a_2, and a_{11},a_{12} exhibit large reciprocal NOEs (Figure 2B,C). This is completely consistent with the COSY peak and confirms a_2, a_{11}, a_{12} as 2-H_α, 2-$H_{\beta c}$, 2-$H_{\beta t}$, respectively; the saturation transfer from set a_i to the sets b_i,c_i similarly yields the 2-vinyl assignments for species B and C. A NOE from the a_{12} (2-$H_{\beta t}$) to 8.1 ppm (not shown) is the same connectivity observed[9] in the model compound of **1** where it was traced to 1-CH_3. Saturation of the low-field resonances a_3 (Figure 4D) and a_4 (Figure 4E) yields NOEs to the apparent methyl peak a_6 and the pair of single proton peaks a_9,a_{10}. The same pattern was observed[9] from the 7-H and 8-H in the same spectral window to the 8-CH_3 and 7-H_αs with the same shifts in the model compound. Hence we assign a_6 to 8-CH_3 and a_9,a_{10} to 7-α-CH_2. The similar NOEs observed for a_3 and a_4 do not allow us to clearly differentiate 7-H from 8-H. All steady-state NOEs and NOESY cross peaks observed could be traced to interaction within the chlorin chromophore; hence no resonances for the protein could be identified.

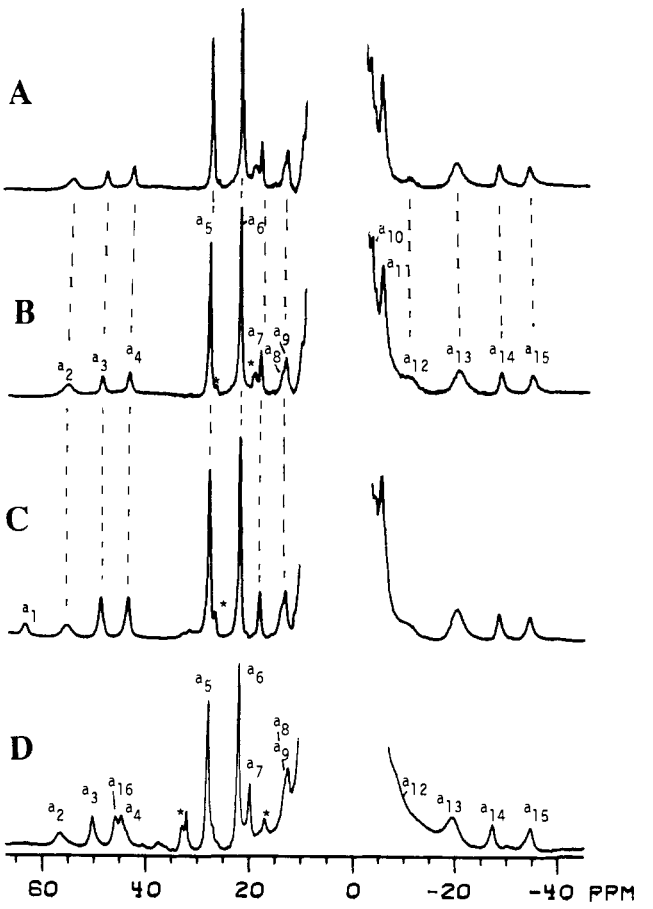

Figure 5. 360-MHz ^1H NMR traces of the deoxy Mb complex of **1** at (A) 35 °C in ^2H_2O, (B) 25 °C in ^2H_2O, and (C) 25 °C in 1:1 ^2H_2O:^1H_2O, all in 0.1 M phosphate, pH 7.0. (D) 360-MHz ^1H NMR spectrum of the deoxy Mb complex of **2** in ^2H_2O, at 25 °C 0.1 M phosphate, pH 7.0. The resonances are labeled a_i; resonances with very similar shifts for the complexes of **1** and **2** are labeled with the same subscript. Impurity peaks are marked with asterisks.

Deoxy Mb Complexes. The 360-MHz ^1H NMR spectra of the high-spin ferrous complex of Mb reconstituted with **1** in ^2H_2O at 35 and 25 °C are shown in Figure 5A,B. Only one set of resonances is clearly observed, a_i, i = 2–4, 7–9, 12, 14, 15 with intensity for single protons, and a_i, i = 5, 6, 11, 13 with area corresponding to methyl groups among the resolved resonances. The chemical shifts at 25 °C, together with the nonselective T_1s, are listed in Table II. Impurity peaks are labeled with asterisks. Comparison of the 25 °C traces of the deoxy Mb complex of **1** in ^2H_2O (Figure 5B) and 1:1 ^1H_2O:^2H_2O (Figure 5C) reveals the existence of a single labile proton, hyperfine shifted peak a_1 at 63.5 ppm, which can be uniquely assigned to the ring labile proton of the axial F8 His.[10,12,13,34] The relative areas of the F8 $N_\delta H$ peak a_1 and γ-*meso*-CH peaks a_3,a_4 (see below), moreover, confirm the 1:1 stoichiometry of the reconstituted complex. The deoxy Mb complex reconstituted with **2** is illustrated in Figure 5D; none of the prominently resolved peaks of the deoxy Mb complex of **1** are lost, although there is an additional peak a_{16} in the complex of **2** which must arise from 2-H. The spectra at various tem-

(33) Parker, W. O., Jr.; Chatfield, M. J.; La Mar, G. N. *Biochemistry* **1990**, *28*, 1517–1525.

(34) La Mar, G. N.; Budd, D. L.; Goff, H. *Biochem. Biophys. Res. Commun.* **1977**, *77*, 104–110.

Table I. NMR Spectral Parameters for Equine Cyano Metmyoglobin Complexes of Chlorins **1** and **2**[a]

peak[b] i in x,	assign	complex of **1**						complex of **2**		
		model[c]	species A			species B	species C	model[c]	species A	species B
		shift[d]	shift[d]	T_1[e]	intercept[f]	shift[d]	shift[d]	shifts[d]	shift[d]	shift[d]
1	5-CH_3	68.2	67.4	6.8	1.4	67.3	73.0	66.4	70.3	*i*
2	2-H_α	42.7	48.9	5.9	5.4	44.5	29.4	[−44.1][j]	[−43.1][j]	[−45.2][j]
3	7-H or 8-H	24.4	32.9	8.1	0.4	31.8	20.1	25.6	29.1	21.4
4	8-H or 7-H	27.7	28.5	8.0	0.8	28.5	14.1	24.0	27.2	*i*
5	*g*		13.1	20					12.9	*i*
	1-CH_3	7.1	8.0	*h*				9.0		
6	8-CH_3	−4.5	−4.6	10				−4.5	−4.3	*i*
7	*g*		−5.0	40					−5.8	*i*
8	*g*		−5.31	5						
9	7-H_α	−5.9	−6.2	10	0.6			−6.0	−7.5	*i*
10	7-H_α	−5.9	−6.5	10	0.6			−6.0	−7.5	*i*
11	2-$H_{\beta c}$	−15.7	−10.1	15	6.1	−15.1	−20.6	−15.7		
12	2-$H_{\beta t}$	−14.4	−11.2	30	7.2	−14.3	−17.6	−15.4		

[a] In ^2H_2O, pH 7.0, 0.1 M phosphate at 25 °C. [b] x_i correspond to sets a_i, b_i, and c_i for species A, B, and C, as given in Figures 1–3. [c] Low-spin, bis-cyano complex. [d] Shifts in ppm, referenced to DSS. [e] Nonselective T_1, in ms; uncertainty ±15%. [f] Apparent intercept at infinite temperatures in a plot of observed shift versus reciprocal temperature, in ppm relative to DSS. [g] Not assigned. [h] Insufficiently resolved to yield T_1. [i] Others of this set likely degenerate with analogous a_i peak. [j] 2-H signal.

Table II. NMR Spectral Parameters for Equine Deoxy Myoglobin Complexes of Chlorins **1** and **2**[a]

peak label[a]	assign	complex of **1**			complex of **2**
		shift[c]	T_1[d]	intercept[e]	shift[c]
a_1	His F8 $N_\delta H$	63.5			62.9
a_2	*β-meso*-H	55.7	2.6	−1	56.9
a_3	*γ-meso*-CH	48.8	14	−6.3	45.9
a_4	*γ-meso*-CH	43.5	12	−5.6	44.8
a_5	5-CH_3	28.0	20	−5.8	
a_6	methyl	22.1	24	1.4	
a_7	single proton	18.1	15	14.4	17.0
a_8	single proton	13.2			12.6
a_9	single proton	10.2			
a_{10}	methyl	−3.41			
a_{11}	methyl	−4.03			
a_{12}	*δ-meso*-H	−10.5	2.2		−5.0
a_{13}	8-CH_3 (?)	−20.1	2	17.6	−19.2
a_{14}	7-H or 8-H	−28.2	9.3	−0.6	−27.4
a_{15}	8-H or 7-H	−34.2	7.3	9.3	−34.8
a_{16}	2-H				42.8

[a] In ^2H_2O, pH 6.9, 0.1 M in phosphate at 25 °C. [b] As labeled in Figures 5 and 6. [c] Shift in ppm, referenced to DSS. [d] Nonselective T_1 estimated for the null ($\tau_{null}/\ln 2 \sim T_1$) in an inversion-recovery experiment; uncertainty ±20%. [e] Apparent intercept, in ppm from DSS, at infinite temperatures in a plot of observed shift versus reciprocal temperature (Curie plot).

peratures do not give evidence for significant peaks for a minor isomer except for the resonance marked with an asterisk in Figure 5B. Hence, the chemical shifts of the various species/impurities are likely more similar and hence obscured by the broader lines.

Reconstitution of the deoxy complex of Mb with **1** deuterated with 5-CH_3, *γ-meso*-CH_2, and (partially) *δ-meso*-H protons affords the NMR trace in Figure 6B, which, upon comparison with the reference trace of Figure 6A, reveals the complete loss of these resonances, methyl a_5 (5-CH_3), and the relatively narrow low-field single proton pair, a_3,a_4, as well as apparent partial loss of the broad, rapidly relaxed upfield shoulder a_{12}. The broad peak a_{12} has a short T_1 that demands it arise from the *δ-meso*-H, leaving the narrow peaks a_3,a_4 as originating from the *γ-meso*-methylene pair. The other broad resonance with T_1 comparable to the *δ-meso*-H a_{12}, namely a_2, is likely also a *meso*-H. Saturation of a_2 leads to an NOE to the assigned 5-CH_3 peak a_5, indicating that a_2 is the *β-meso*-H (Figure 6C). Irradiation of a_3 leads to a ~20% NOE at a_4 (Figure 6D), which, with the measured $T_1 \sim 20$ ms, confirms[33] that a_3,a_4 is a geminal pair from the *γ-meso*-CH_2. Saturation of the upfield single proton peak a_{14} (Figure 6F) does not lead to a detectable NOE (i.e. <5%) to any other resonance (specifically to a_{15}) and hence excludes the pair of single resonances a_{14},a_{15} as arising from a methylene group. Since the minimal

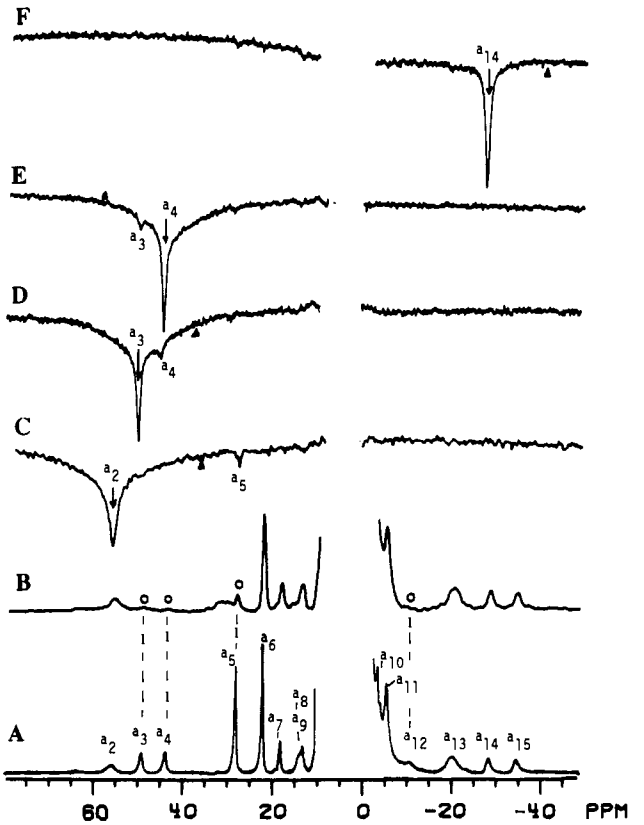

Figure 6. (A) 360-MHz ^1H NMR reference trace of the deoxy Mb complex of **1** in ^2H_2O, 0.1 M phosphate, pH 7.0. (B) ^1H NMR spectrum under the same conditions as above for the deoxy Mb complex of **1** deuterated at the 5-CH_3, *γ-meso*-CH_2, and *δ-meso*-H positions; note loss (marked o) of intensity of methyl peak a_5 (5-CH_3), the narrow pair of peaks a_3,a_4 (*γ-meso*-CH_2), and the broad upfield shoulder a_{12} (*δ-meso*-H). (C–F) NOE difference traces obtained by saturating the desired resonance (marked by arrow) and subtracting it from a trace where the decoupler is placed well off-resonance; the position of the off-resonance decoupler is marked by a solid triangle. (C) Saturate peak a_2; note NOEs to methyl peak a_5 (5-CH_3). Saturate peak a_3 (D) and a_4 (E); note reciprocal NOEs. (F) Saturate peak a_{14}; note the absence of a NOE to any resolved resonance, in particular to a_{15}.

magnetic anisotropy of high-spin iron(II) systems leads to small dipolar shifts for noncoordinated residues in the heme pocket,[10,12,21] the pair of peaks a_{14},a_{15} must arise from the prosthetic group but cannot arise from the 2-vinyl (peaks are retained in the deoxy Mb complex of **2**; see Figure 5F), 7-*α*-CH_2, 7-*β*-CH_2, or 4-*α*-CH_2 (all geminal pairs). This leaves 7-H and 8-H as the only candidates

for peaks a_{14},a_{15}. A likely candidate for the broad upfield methyl peak a_{13} is 8-CH_3. The methyl or the saturated ring has been found to be much more strongly relaxed than the other methyls in the low-spin sulfmyoglobin complexes.[35]

Discussion

metMbCN Electronic Structure. The present data on the metMbCN complex do not shed any direct light as to the orientation of the iron(III) pyropheophorbide *a* (**1**) in the pocket of Mb. This is due to the failure to detect any hyperfine shifted protein signals such as Phe CD1 or Ile FG5, which would provide a reference point for locating the side chains of the chromophore in the pocket.[36,37] The apparently much smaller dipolar shifts for the metMbCN complex of **1** are due to the reduced magnetic anisotropy, as is clearly reflected in the low-temperature *g* values whose spread is significantly reduced below that of the native protein. Previous NMR studies[19] of the Zn(II) complex of the free acid of **1** had shown that the E7 Val ring current shift was indicative of an orientation that is the same as that for native protohemin. There is no evidence to conclude that the major component of the iron complex has an orientation of **1** in the pocket different from that of the Zn(II) complex.

The major component A with peaks a_i, as well as species B with peak b_i, exhibit a methyl/vinyl hyperfine shift pattern essentially identical to that of the low-spin bis-cyano model compound[9] of **1**, as shown in Table I. Thus the π spin delocalization occurs in the $3e_\pi(xz)$ (large shifts on pyrroles cis to the saturated ring) and former a_{1u} orbitals (low-field 7-H, 8-H contact shifts), as discussed in detail previously[9] for the model compound of **1**. The metMbCN complex of **2** also exhibits a hyperfine shift pattern remarkably close to that of the bis-cyano complex of **2**. The lack of a major protein perturbation on the spin distribution of **1** or **2** in species A or B of metMbCN relative to the bis-cyano model complexes (Table I) is completely consistent with the chlorin of the major components occupying the same orientation in the protein matrix as protohemin. This is due to the fact that the Mb matrix, by virtue of the His F8 imidazole orientation, stabilizes π spin density in the same $3e_\pi(xz)$ component in an axially symmetric hemin;[9,12] hence the two rhombic perturbations are collinear and additive, and the incorporation into the proton matrix of **1** does not further reduce the symmetry of the electronic structure. The essential identity of the contact shift pattern of the sulfhemin-C in $metS_cMbCN$[35] and its extracted bis-cyano complex[38] was similarly interpreted on the basis of colinear rhombic perturbations; sulfhemin-C is a chlorin with pyrrole B saturated. Thus the ^1H NMR contact shift pattern of a low-spin ferric chlorin protein will yield little useful information on the binding pocket if the axial His orientation is along the N–Fe–N vector through the saturated pyrrole.

However, the strong perturbation of the skeletal π spin density of species C of the metMbCN complex of **1** argues that the rhombic perturbations on the electronic structure of the tetrapyrrole due to ring D saturation and the protein matrix (i.e. His orientation) are not colinear, and hence indicate an orientation of **1** in C that is different from that of species A or B. This suggests that the unpaired spin distribution and orbital ground state of an iron chlorin may be significantly perturbed upon incorporation into a protein matrix if the orientation of the rhombic perturbation due to the protein does not coincide with the N–Fe–N vector through the saturated pyrrole. The low concentration and broad lines prevented the detection of a distinct set of ESR lines which could be attributed to species C.

Protein Heterogeneity. The three species A, B, and C, which give rise to sets of peaks a_i, b_i, and c_i for the metMbCN complex of **1**, are clearly readily interconvertible forms of the same complex. The two species with peaks a_i and b_i reflect very similar electronic structures. For 5-CH_3 (a_1,b_1) and 7-H/8-H (a_3,b_3/a_4,b_4), the pairs of resonances are essentially degenerate, with the major difference between the two species reflected in the vinyl peaks, for which the b_i peaks exhibit an upfield bias of 3–4 ppm relative to the a_i peak. However, the interconversion between sets of peaks a_i,b_i does not involve simply a change of vinyl orientation, since the same pattern of peaks is found in the metMbCN complex of **2** which has the vinyl group removed. Rather, the two species must reflect some minor conformational differences for an amino acid side chain, and the influence on the heme of the conformational heterogeneity is a change in the mean vinyl orientation. Studies on model compounds and proteins have shown[39] that largely in-plane vinyl groups exhibit large H_α/H_β contact shift ratios and that a more out-of-plane orientation leads to a sharp reduction in the ratio. The selective upfield bias of both H_α and H_β contact shifts for the species B indicates a 2-vinyl group that is more out-of-plane in species B than A. However, the essentially identical contact shifts for the remaining substituents argue against a significant difference in the electronic and hence molecular structure of the active site in species A and B.

The third equilibrium species, C, with peaks c_i, however, appears to reflect a significantly perturbed spin density distribution, with both the vinyl and other resolved resonances (in particular 7-H/8-H peaks c_3/c_4) exhibiting a spin distribution pattern quite different from that of either species A or B. Since the interconversion between forms C and A or B is on the ~20 ms time scale, heme reorientation about the α,γ-meso axis, is very unlikely, since such reorientation requires breaking both the Fe–His and Fe–CN bonds, and has been shown[40] to occur with lifetime >1 h for hemes, some 10^5 slower than the present interconversion rate. However, variable orientations of the hemes relative to the protein matrix are accessible without bond breaking or heme dissociation, simply by reorientation about the intact Fe–His bond. Such reorientations have been documented[37,41] in numerous Mb complexes containing hemes with altered carboxylate side chains, specifically a hemin possessing only a single propionate side chain,[37] and the interconversion rates found to be in the ~10 ms time scale. The very similar interconversion lifetime observed here supports the hypothesis that species C has the heme rotated by 90° from that in species A or B. Since the present NMR experiment could not uniquely establish the orientation of the chlorin in species A, we restrict ourselves at this time to the conclusion that species C differs from A/B by a 90° rotation about the Fe–His bond.

A similar labile heterogeneity has been observed by ^1H NMR spectroscopy in the diamagnetic sperm whale Mb complexes of several Zn chlorins.[19] However, a definitive comparison of the presently observed dynamic heterogeneity in the iron complex of **1** in equine Mb with that previously reported for the Zn(II) complex of the free acid of **1** in sperm whale Mb is not possible at this time. Differences in the ligation state and esterification of the propionate side chain could strongly modulate both the thermodynamics and dynamics of such equilibrium heterogeneities. The two Zn-chlorin-Mb species were concluded[19] to differ not in the orientation of the chlorin but in a slight conformation of the protein environment. Moreover, the interconversion lifetime was found to be of the order of 1 to 10^2 s, much slower (by $>10^2$) than that presently observed between species A and B in the iron complex of **1**. The population of a third species for the iron complex of **1** could arise because esterification stabilizes the location of the propionate side chain in the more hydrophobic protein interior. It is also possible that additional species exist for the Zn(II) complex of the free acid of **1** but that the limited chemical shift range in the diamagnetic complex prevents detection

(35) Chatfield, M. J.; La Mar, G. N.; Smith, K. M.; Leung, H.-K.; Pandey, R. K. *Biochemistry* **1989**, *27*, 1500–1507.
(36) La Mar, G. N.; Emerson, S. D.; Lecomte, J. T. J.; Pande, U.; Smith, K. M.; Craig, G. W.; Kehres, L. A. *J. Am. Chem. Soc.* **1986**, *108*, 5568–5573.
(37) Hauksson, J. B.; La Mar, G. N.; Pandey, R. K.; Rezzano, I. N.; Smith, K. M. *J. Am. Chem. Soc.* **1990**, *112*, 6198–6205.
(38) Chatfield, M. J.; La Mar, G. N.; Parker, W. O., Jr.; Smith, K. M.; Leung, H.-K.; Morris, I. K. *J. Am. Chem. Soc.* **1988**, *110*, 6352–6358.
(39) La Mar, G. N.; Viscio, D. B.; Gersonde, K.; Sick, H. *Biochemistry* **1978**, *17*, 361–367.
(40) La Mar, G. N.; Toi, H.; Krishnamoorthi, R. *J. Am. Chem. Soc.* **1984**, *106*, 6395–6401.
(41) Hauksson, J. B.; La Mar, G. N.; Pandey, R. K.; Rezzano, I. N.; Smith, K. M. *J. Am. Chem. Soc.* **1990**, *112*, 8315–8323.
(42) La Mar, G. N.; Budd, D. L.; Sick, H.; Gersonde, K. *Biochem. Biophys. Acta* **1978**, *533*, 270–283.

of such small concentration. The detection of the various species in the paramagnetic, low-spin iron(III) complex is greatly facilitated by the vastly expanded chemical shift scale and the exquisite sensitivity of hyperfine shifts to protein environment. This large shift scale, moreover, facilitates not only detection but also temporal resolution. Thus the same interconversion lifetimes (20 ms) currently observed would average shift differences of <0.5 ppm and hence would lead to only a completely time-averaged ^{1}H NMR spectrum of the three species for a diamagnetic complex.

The fact that the heterogeneity is not clearly detected in the high-spin iron(II) Mb complex of **1** suggests the possibility that the thermodynamics and/or dynamics of the heterogeneity depend on the ligation/oxidation state. Whether the interconversion is faster in the five-coordinate iron(II) Mb complex or the population of the minor species decreased cannot be determined from the present data. The present study, however, suggests that chlorins may adopt alternate orientations in the pocket of Mb that differ by 90°, and hence interfere with the unique determination of the polarization of transitions in the Mb matrix.

Deoxy Mb Electronic Structure. The dominant contact shifts of the high-spin ferrous state provide direct information on bonding to the iron as well as on its electronic orbital ground state.[10,12,13,21] Large contact shifts at meso positions are indicative of π-spin delocalization into vacant π molecular orbitals in both porphyrins[10] and chlorins.[38] For a chlorin, moreover, large contact shifts can be expected for the saturated ring 7-H and 8-H if there is π bonding to the filled former a_{1u} orbital of a heme.[9,16] Inspection of the ^{1}H NMR spectra of the deoxy Mb complexes of **1** and **2** reveals the largest contact shifts for meso substituents and the 7-H, 8-H pair (Table II), establishing the presence of extensive π bonding not only with the former a_{1u} orbital, as found for the low-spin ferric state,[9] but also with the vacant A_6*,S_8*, the analogs of the heme $4e_\pi$* orbitals.[9,10] The ^{1}H NMR spectra of high-spin ferrous model hemes[10] and native deoxy Mb[2] reveal only minimal contact shifts for meso substituents, and hence do not provide direct evidence for π back-bonding in hemes. Thus a chlorin appears to serve as a better π acceptor than a porphyrin in the high-spin ferrous state.

The pattern of the meso substituent and 7-H/8-H contact shifts, moreover, provides insight into the orbital ground state. Various theoretical approaches had predicted an orbital ground state[43] $(xy)^2(xz)(yz)(z^2)(x^2-y^2)$ or one of the pair[44-46] $(xz)^2(yz)(xy)(z^2)(x^2-y^2)/(yz)^2(xz)(xy)(z^2)(x^2-y^2)$. Positive π-spin delocalization into the π antibonding orbital leads to upfield *meso*-H and low-field *meso*-CH_2 contact shifts and into the former a_{1u} orbital leads to downfield 7-H/8-H contact shifts.[9,10,47] The deoxy Mb complex of **1**, however, exhibits positive π-spin density only at δ-*meso*-H and γ-*meso*-CH_2 and *negative* π-spin density at β-*meso*-H and 7-H/8-H. The delocalization of negative π-spin density occurs only if the participating metal d orbital is filled,[47] and therefore one of the two metal π-bonding orbitals, d_{xz} or d_{yz}, must be filled. Hence the orbital ground state with doubly occupied d_{xy} can be eliminated. This conclusion is consistent with both ab initio SCF calculations[46] and crystal-field interpretation[45] of Mössbauer and magnetic susceptibility data on deoxy Mb.

For the conserved axial His F8, the ring labile proton has been shown to serve as an indicator of the Fe–imidazole σ bonding, where a weakening of the bond is reflected in a decreased $N_\delta H$ contact shift.[13] The His F8 $N_\delta H$ contact shift in the deoxy Mb complex of **1** is some 12 ppm smaller than in deoxy Mb possessing a heme.[34] Moreover, its shift is the same in the complex of chlorin **1** as for the deoxy Mb complex of various sulfhemins,[48] all of which are iron chlorins. A similar 12-ppm decrease in His F8 $N_\delta H$ contact is observed for each subunit of deoxy Hb upon substituting the hemins by an iron sulfhemin.[49] Thus the reduced axial covalency appears to reflect a characteristic difference in the equatorial bonding of a chlorin relative to a heme.

Acknowledgment. The results were supported by grants from the National Institutes of Health (GM 26226 and HL 22252).

Supplementary Material Available: Table giving chemical shifts of the low-spin ferric bis-cyano complexes of **1** and **2** (1 page). Ordering information is given on any current masthead page.

(43) Trautwein, A.; Eicher, H.; Meyer, A.; Alfsen, H.; Waks, M.; Rosa, J.; Baizard, Y. *J. Chem. Phys.* **1970**, *53*, 963–967.

(44) Trautwein, A.; Zimmermann, R.; Harris, F. E. *Theor. Chem. Acta* **1975**, *37*, 89–103.

(45) Huynh, B. H.; Papaethymiou, G. C.; Yen, G. S.; Groves, J. L.; Wu, C. S. *J. Chem. Phys.* **1974**, *61*, 3750–3758. Eicher, H.; Bade, D.; Parak, F. *J. Chem. Phys.* **1976**, *64*, 1446–1455.

(46) Rohmer, M.-M.; Dedieu, A.; Veillard, A. *Chem. Phys.* **1983**, *77*, 449–462.

(47) La Mar, G. N. In *NMR of Paramagnetic Molecules*; La Mar, G. N., Horrocks, W. D., Jr., Holm, R. H., Eds.; Academic Press: New York, 1973; pp 85–126.

(48) Chatfield, M. J.; La Mar, G. N.; Kauten, R. J. *Biochemistry* **1987**, *26*, 6939–6950.

(49) Chatfield, M. J.; La Mar, G. N. *Arch. Biochem. Biophys.* **1992**, *295*, 289–296.